

LANDSLIDE SUSCEPTIBILITY ASSESSMENT BY TRIGRS IN A FREQUENTLY AFFECTED SHALLOW INSTABILITY AREA

Mariantonietta Ciurleo*, Maria Clorinda Mandaglio*, Nicola Moraci*

*Department of Civil, Energy, Environmental and Materials Engineering, "Mediterranea" University of Reggio Calabria, Via Graziella - Loc. Feo di Vito - 89122 Reggio Calabria (RC)

Corresponding author: Nicola Moraci (email: nicola.moraci@unirc.it). Department of Civil, Energy, Environment and Materials Engineering (DICEAM), Mediterranean University of Reggio Calabria, Reggio Calabria, Italy

ABSTRACT

Landslide susceptibility assessment over large areas is considered a preliminary step for the planning or design of the most appropriate risk mitigation measures. The use of physically-based models is considered a useful tool for landslide susceptibility assessment. Sometimes, using the available geotechnical input data, physically-based models can be used to assess landslide susceptibility to obtain a susceptibility map which allows the expert to identify areas where detailed in situ investigations and laboratory tests should be carried out.

In this context, the paper proposes a methodology based on the use of TRIGRS to assess landslide susceptibility in an area of about 1 km² frequently affected by shallow phenomena in weathered gneiss. Owing to the fact that these materials are extremely complex to characterize from a mechanical and hydraulic point of view, the methodology starts with the collection and analysis of the geotechnical data available for weathered gneiss outcropping in the study area. These data are combined with the data provided by scientific literature on soils similar, for genesis and stress history, to those of the studied area. Through the application of TRIGRS, the data are combined in order to obtain the values of parameters that better analyze shallow landslide source areas. Subsequently, using the above-mentioned values, several susceptibility maps are obtained. Finally, the most representative shallow landslide susceptibility map for the area is chosen by means of the error index (EI), the true positive fraction (TPF) and the Forecasting Index (FI). The success of the best map is confirmed by the high value of the Area Under the receiver operator characteristic Curve (AUC) that demonstrates a good level of forecasting ability.

Keywords: weathered gneiss, shallow landslides, susceptibility, TRIGRS

INTRODUCTION

Rainfall-induced shallow landslides are common on steep natural hillslopes mantled with a layer of colluvium or residual soil (Salciarini et al. 2006). They may evolve in flow-like landslides, presenting high velocities, and can cause loss of human life and severe socio-economic disasters (Hungar et al. 2014).

In weathered crystalline rocks, these phenomena present failure surfaces generally located along the contact between residual or colluvium soils and relatively less weathered rock (Borrelli et al. 2015, 2016). Due to their heterogeneity and the difficulty of undisturbed sampling, the geotechnical characterization is highly complex, and, as a consequence, experimental studies on naturally weathered rocks are limited (Gullà et al. 2005, 2006; Mandaglio et al. 2016a). In this context, shallow landslide susceptibility assessment in weathered rocks over large areas is also extremely complex. The susceptibility assessment of these phenomena can be carried out using the few detailed available data and the data provided by scientific literature on soils similar for genesis and weathering grade. The relevance of shallow landslide consequences makes the susceptibility assessment fundamental, especially for the planning of the most appropriate risk mitigation measures (Borrelli et al. 2018; Mandaglio et al. 2015, 2016b; Giofrè et al. 2017).

The best known definition of landslide susceptibility was proposed by Brabb (1984) who, starting from the principle that the past and present are keys to the future (Varnes, 1984), underlined the forecasting ability of susceptibility maps (Calvello et al. 2013). Later, Fell et al. (2008) defined landslide susceptibility as a quantitative or qualitative assessment of the classification, volume (or area) and spatial distribution of existing and potential landslides in a study area. This goal can be pursued by applying different zoning methods available in scientific literature. Soeters and van Westen (1996) classified these methods as heuristic, statistical and deterministic. Heuristic methods, able to process essentially topographic and geological input data, are considered basic methods for both analysing existing, and forecasting potential landslides (Cascini 2008). When further details on input data are added and procedures based on statistical analysis are used, the methods are considered intermediate (Cascini 2008). Finally, deterministic methods need hydrogeological and geotechnical data and are considered advanced methods (Cascini et al. 2008). According to these considerations, using advanced methods such as a physically-based model, able to reproduce the physical processes governing landslide triggering (e.g. Sorbino et al. 2010; Ciurleo et al. 2017; Moraci et al. 2017), the landslide susceptibility zoning of an area can be obtained.

One of the most widely used physically based models is the Transient Rainfall Infiltration and Grid-based Slope-Stability model TRIGRS (Baum et al. 2002; Savage et al. 2004). This model relies on the combination of an infiltration model, for

This is a post-peer-review, pre-copyedit version of an article published in journal *Landslide*. The final authenticated version is available online at <https://doi.org/10.1007/s10346-018-1072-3>

pore water pressure analysis, with an infinite slope stability model for the computation of the Safety Factor (e.g., Baum et al. 2005; Montrasio et al. 2011; Salciarini et al. 2017). Despite the ability of the model to analyse shallow landslide triggering over broad areas, it requires representative, spatially distributed geotechnical properties of soils; a correct initial water table location; soil thickness; topographic, geological and rainfall data.

The paper aims to assess the susceptibility of shallow landslide source areas in weathered gneiss by TRIGRS. The method is tested on a large scale (1:5000) in a study area located in southern Italy, periodically affected by shallow landslides, some of which evolve into debris flows. The paper preliminarily focuses on the identification of geotechnical and hydraulic properties of soils affected by shallow landslides thus allowing the identification of the input data. To carry this out, all the available geotechnical and geological information on weathered gneiss outcropping on the study area, and the data available in the surrounding zones or in other geographical contexts – characterised by soils similar from a geological and a geotechnical point of view – were summarised and used as input data for TRIGRS. Finally, several parametric analyses were performed by TRIGRS thus obtaining several susceptibility maps which are then compared and critically analysed in order to identify the best map.

2. STUDY AREA AND GEOTECHNICAL DATA

The study area (Fig. 1) is located between Bagnara Calabria and Scilla, along the SW coast of the Calabria region (Southern Italy). It is strictly linked to the geological context of the Messina Strait (Ferranti et al. 2008) and falls within the southern border of the Calabrian–Peloritani arc.

The study area, about 1 km², is bordered at the top (630 m a.s.l.) by a flat surface of marine origin (Piano delle Aquile), and at the bottom (0 m a.s.l.) from a densely urbanized coastal plain, where the village of Favazzina is located (Fig. 2). The slopes are crossed by the A3 (SA-RC) highway, the railway and the SR 18 southern Tyrrhenian state road (Fig. 2). The slopes are characterised by a Paleozoic basement, made up of high-grade metamorphic rocks (para and ortho-gneiss), overlapped by Upper Pliocene to Holocene sedimentary deposits (Borrelli et al. 2012; Giofrè et al. 2016).

The Paleozoic crystalline basement shows intense and deeply weathered conditions (Fig. 2). Particularly, residual, colluvial and detrital soils (Class VI), classified according to GCO (1988) and Borrelli et al. (2014, 2015, 2016), cover about 60% of the study area. Completely weathered rocks (Class V) prevail in the upper portion of the slope, while highly and moderately weathered rocks (respectively, Classes IV and III) crop out in the middle-lower portions of the slope (GCO, 1988; Borrelli et al. 2014, 2015, 2016).

The study area has been frequently affected by shallow landslides of flow type and, particularly in the last decade, shallow landslides have been triggered on class VI and during the run-out phase, severely affecting the urbanized area and transportation infrastructures located along the coastal plain (Fig. 2).

Among these, the most insidious phenomena occurred in 2001 and 2005. The first took place on 12th May 2001 and involved the methane pipeline, while the second occurred on 31th March 2005 on the slope overlooking the village of Favazzina (Fig. 2).

In both cases, these phenomena can be classified as very rapid to extremely rapid debris flows. They struck Favazzina, the SNAM (European gas utility public company) station of the methane pipeline, the SA-RC highway, the SR 18 state road, and the railway causing the derailment of the intercity trains Turin-Reggio Calabria (2001 event) and Reggio Calabria-Milan (2005 event).

These phenomena initially began as translational landslides located in the head of the channels, immediately below the secondary road, and affected the residual soils (Class VI) with a slip surface located at a depth generally less than 2 metres.

Data provided by Antronico et al. (2006) on the weathered gneiss of Class VI of Favazzina slopes were collected and combined with new in situ investigations and laboratory tests carried out in the study area. The overall available information consisted of: the stratigraphic conditions of the source areas; the grain size distribution, physical properties of soils and the mechanical properties of weathered gneiss in saturated conditions.

Referring to stratigraphic conditions, some information about the thickness of class VI was provided by three seismic refraction prospects and six continuous drilling boreholes (Fig. 3).

The in situ investigations showed the spatial variability of weathered soils thicknesses (Class VI) ranging from 1.4 m to 4.6 m depth (Fig. 3). Particularly, in the upper part of the slope (where shallow landslide source areas were located), the thickness of class VI assumes a value ranging from 1.5 m (Fig. 3, S2) to 2.0 m (Fig. 3, S1) while its value ranges from 1.4 m to 4.6 m, in the middle portion of the slope (Fig. 3, S3, S4, S5, S6). These values have been confirmed by seismic refraction prospects (ST1, ST2 and ST3) that show an average value of thickness ranging from 2 m to 5 m (Fig. 3).

In the study area, soils of class VI can be classified as silty sand (SM) with the following fractions; sand = 50.58%, gravel = 27.26%, silt = 19.05% and clay = 3.11% and as inorganic silt of medium compressibility with sand (ML) with fractions of Sand = 30 %, Silt = 45%, Clay = 25%, according to the Unified Soil Classification System (USCS). The plastic index and liquid limit of the sampled soil are 9.23 % and 33.27%, respectively. Regarding the physical properties of class VI, the natural unit weight values (γ) range from 15 kN/m³ to 20 kN/m³; the saturated unit weight (γ_{sat}) varies from 19 kN/m³

to 22 kN/m³; the dry unit weight (γ_d) ranges between 12.5 kN/m³ and 16 kN/m³; the void ratio (e) is variable from a minimum of 0.65 to a maximum of 1.15; the values of soil porosity (n) vary from 0.4 to 0.54 and the degree of saturation (S) from 43% to 99% (Antronico et al. 2006).

The results of direct and triaxial tests carried out on these soils have shown that the shear strength envelope ranges from an upper limit, with a cohesion value of 0 kPa and a shear strength angle of 44°, to a lower limit characterized by a cohesion value of 0 kPa and a shear strength angle of 38°.

For rainfall data, the only available information can be gathered by the Scilla rain gauge of the Centro Funzionale Multirischi—ARPACAL (Calabria Region) (cod. 2510 — located near the study area), with reference to two shallow landslide triggering dates, 12 May 2001 and 31 March 2005. The rainfall data were, respectively, equal to 20 mm over two consecutive days on 12 May 2001 and 13.6 mm over two consecutive days on 31 March 2005.

3. DATABASE AND METHODOLOGY

3.1 Methodology

The methodology used for the susceptibility assessment of shallow landslide source areas in weathered gneiss can be divided into two stages. The first stage is used for data base creation in order to identify the values of the input parameters to be applied in the second stage. The second stage consists in the calibration of the physically based TRIGRS model for the assessment of the susceptibility to shallow landslide source areas at large scale (1:5000).

The first stage was carried out by collecting all the available information on the soils affected by shallow landslides in the study area, i.e. weathered gneiss of class VI.

Since few detailed in-situ investigations and laboratory tests are available for the soils of class VI of the studied area, a geotechnical data base was created combining the data provided by scientific literature on soils similar, for genesis and stress history, to those of the studied area with available data.

The main goals of this stage were to: i) identify and sum up ranges of variation of the main geotechnical properties of gneiss of class VI; ii) identify the thickness of class VI; and iii) localize the initial pore water pressure conditions.

In the second stage, shallow landslide susceptibility maps by means of TRIGRS were obtained by varying the geotechnical input data in the ranges previously identified.

TRIGRS is a physically-based model widely used for computing the triggering areas of rainfall induced shallow landslides in different geo-environmental contexts (Godt et al. 2008; Schilirò et al. 2015; Sorbino et al. 2010). TRIGRS couples an infiltration model with an infinite slope stability model. The infiltration model in TRIGRS is based on the use of the linearized solution of the Richards equation proposed by Iverson (2000) and extended by Baum et al. (2002) to the case of an impermeable bedrock located at a finite depth.

TRIGRS predicts the pore-water pressure regime in saturated conditions using the following input parameters: slope, soil cover depth, depth of the initial steady-state water table, the steady (initial) surface flow and saturated hydraulic conductivity (K_s).

The original TRIGRS code, as developed by Baum et al. (2002) for fully saturated conditions, was later extended by Baum et al. (2008) to unsaturated soils (Salciarini et al. 2017). TRIGRS predicts pore-water pressure regime in unsaturated/saturated conditions, coupling the simple analytic solution for transient unsaturated infiltration proposed by Srivastava and Yeh (1991) to the original TRIGRS equation (Baum et al. 2008; Savage et al. 2004). This model is based on the fitting equation of soil water characteristic curve proposed by Gardner (1958) depending on four hydraulic parameters: saturated soil water content (θ_s), residual soil water content (θ_r), saturated hydraulic conductivity (K_s) and the Gardner parameter (α). The infiltrating water accumulates at the base of the unsaturated zone and then rises to the ground surface.

In both cases, the model approximates the infiltration process as a one-dimensional vertical flow and the obtained results are highly sensitive to the initial seepage condition.

The stability of an individual grid cell is analyzed by the one-dimensional infinite-slope model proposed by Taylor (1948) for the calculation of the safety factor in the unsaturated configuration, as follows:

$$F_s(Z, t) = \frac{\tan\phi'}{\tan\delta} + \frac{c' - \Psi(Z, t)\gamma_w \tan\phi'}{\gamma_s Z \sin\delta \cos\delta} \quad (1)$$

where:

c' is soil cohesion for effective stress, ϕ' is soil shear strength angle for effective stress, δ is slope gradient, $\Psi(Z, t)$ is the ground water pressure head ($\Psi = u/\gamma_w$), depending on Z (vertical coordinate direction) and t (time), γ_w is unit weight of groundwater, γ_s is soil unit weight.

To compute the safety factor above the water table, the matric suction, $\Psi(Z, t)\gamma_w$, is multiplied by χ , Bishop's (1959) effective stress parameter. According to Vanapalli and Fredlund (2000), χ can be approximated as:

$$\chi = \frac{(\theta - \theta_r)}{(\theta_s - \theta_r)} \quad (2)$$

This is a post-peer-review, pre-copyedit version of an article published in journal Landslide. The final authenticated version is available online at <https://doi.org/10.1007/s10346-018-1072-3>

where:

θ is the volumetric water content, θ_r is the residual water content, and θ_s is the water content at saturation.

This analysis allows the calculation of the safety factor in each cell of the domain in which the study area is discretized. Moreover, the analysis is sensitive to some of the required input data, such as hydraulic properties of soils, initial steady-state groundwater conditions and soil depths (Godt et al. 2008; Salciarini et al. 2006; Sorbino et al. 2007, 2010).

TRIGRS, combined with a geographic information system (GIS), allows us to distinguish unstable ($FS \leq 1$) from stable cells ($FS > 1$).

In order to quantify TRIGRS results, in both saturated and unsaturated conditions, and to evaluate the performance of the model in the forecasting of shallow landslide source areas, the error index (EI) was used (Fig. 4). EI is defined, as follows:

$$EI (\%) = \frac{A_{TL} - A_{UTL}}{A_{TL}} = \frac{\sum Cells_{TL} - (\sum Cells_{TL} \cap \sum Cells_{FS \leq 1})}{\sum Cells_{TL}} \quad (3)$$

Where A_{TL} are the landslide source areas according to the landslide inventory (observed source areas), A_{UTL} areas computed as unstable located within the A_{TL} (observed source areas), $\sum Cells_{TL}$ summation of cells actually affected by landslide source areas according to the landslide inventory, $\sum Cells_{FS \leq 1}$ summation of cells computed as unstable by the model.

EI is the complementary of the true positive fraction of the model (TPF), also called *sensitivity*.

In order to evaluate the model forecasting capacity, the forecasting index (FI) was used (Fig. 4). FI is defined, as follows:

$$FI (\%) = \frac{A_{UN} - A_{UTL}}{A_{ST}} = \frac{\sum Cells_{FS \leq 1} - (\sum Cells_{TL} \cap \sum Cells_{FS \leq 1})}{\sum Cells_{ST}} \quad (4)$$

where: A_{UN} areas computed as unstable, A_{ST} the area of the basin not affected by triggering phenomena, $\sum Cells_{ST}$ summation of cells not affected by landslides according to the landslide inventory.

Herein FI is considered a forecasting index in order to define the areas potentially affected by landsliding but unaffected by shallow landslide source areas until now. The equation 4 was originally defined “*false positive proportion/fraction (FPF or 1-Specificity)*” by Metz (1978) and Swets (1988), and actually used in statistical studies by several authors (e.g., Calvello et al. 2013; Fressard et al. 2014; Calvello and Ciurleo 2016; Ciurleo et al. 2016).

3.2 Database

Tables 1 and 2 summarize the geotechnical and hydraulic properties of class VI weathered gneiss gathered in the first stage of the methodology. In particular, the saturated unit weight values (γ_s) range from 19.22 kN/m³ to 21.98 kN/m³; the cohesion value ranges from 0 kPa to 5 kPa and the shear strength angle from 30° to 44°, Table 1.

Regarding hydraulic properties, due to the lack of data for the study area, the values proposed by Gullà and Sorbino (1994); Cascini et al. (2006); Calvello et al. (2008) and Schilirò et al. (2015), obtained from laboratory (Richards pressure plate) and in situ tests (permeability tests) performed on gneiss similar for genesis and weathering grade (Class VI), were used in this study (Tab. 2). In particular, Gullà and Sorbino (1994), Calvello et al. (2008) and Cascini et al. (2006) identified for gneiss of class VI of the Unit of Sila (Calabria) saturated permeability values (K_s) ranging from 1.27E-06 m/s to 3.50E-05 m/s; and Schilirò et al. (2015) identified, for gneiss of class VI of the Unity of Aspromonte (Sicily), saturated permeability values varying from 7.91E-06 m/s to 6.60E-05 m/s, the same authors also provided indications on the values of saturated volumetric water content θ_s , ranging from 0.38 to 0.39, and of saturated hydraulic diffusivity coefficient $D_0 = 1.55E-04$ m²/s – 3.84E-04 m²/s.

Regarding the initial pore water pressure condition, general information was provided by investigations and studies developed in weathered gneiss by Gullà and Sorbino (1996). The authors showed that at a depth of 1.45 m, the tensiometer measurements had values close to 0 in the months between February and May 1994 where shallow landslides of flow type occurred.

Referring to rainfall data, it was decided to consider the most intensive rainfall event - equal to 20 mm over two consecutive days on 12 May 2001 - in order to simulate the most critical conditions.

The overall data collected in the first stage were used as input parameters of TRIGRS in the second stage.

Other input data employed within TRIGRS are the following: digital elevation model (DEM), flow direction, cover depth, initial water table location. The spatial data are expressed in raster format using 5×5 m² square grid cells, and flow direction was directly derived by DEM.

Considering the presence of a thin layer of class VI over the parent material, a finite depth for the impermeable basal boundary was assumed. In this regard, a constant soil thickness equal to 1.5 m was considered. This assumption errs on the side of caution and is coherent with borehole logs S1 and S2 (Fig. 3) that underline a thickness of soil of class VI ranging from 1.5 m (S2) to 2.0 m (S1) in the upper part of the slopes where shallow landslides triggered in 2001. Furthermore, within the source areas of the shallow landslides triggered on 12 May 2001 and 31 March 2005, the

geomorphological evidence shows 1.5 m slip surfaces located at the contact between the soil of class VI and the underlying bedrock.

With reference to the initial water table, different locations depending on the different cases of analysis were taken into consideration. The first was implemented locating the water table at the contact between the class VI and the parent rock in the whole study area. This assumption is coherent with the data provided by Gullà and Sorbino (1996) and summarized above. The second was implemented considering the influence of the secondary road in the upper part of the basin in the 2001 shallow landslides. To do this, a buffer zone constituted by three contour lines, each equal to 5 m, below the secondary road and two different locations of the water table, respectively at 0 m and 0.5 m from the ground surface, were considered (Fig. 5).

4. ANALYSES OF THE RESULTS

The study area was analyzed by TRIGRS and parametric analyses were performed (Table 3) according to 36 different cases in saturated and unsaturated conditions. Table 3 summarizes the parameters used for the modelling, the first column reports a progressive identification number and the letter S, indicative of total saturation condition, or U for unsaturated conditions.

In all cases, a constant value of soil thickness equal to 1.5 m of depth from the ground surface, the average value of hydraulic data, an initial steady state water table located at the bedrock–soil interface, in the whole study area, except in the road buffer zone (zone “A” in Fig. 5) was assumed. In zone “A”, parametric analyses that consider a depth of water table located at 1.5 m, 0.5 m and 0 m from the ground surface were carried out in order to simulate the influence of the road on shallow landslide triggering. It is worth mentioning that in the cases where the water table in “zone A” is assumed equal to 0 m, TRIGRS in unsaturated conditions works equally to TRIGRS (i.e. the safety factor was evaluated considering $\Psi = 0$ at the ground surface and χ Bishop’s (1959) equal to 1). On the contrary, in the remaining study area (zone B, Figure 5) unsaturated TRIGRS considers different values of Ψ and χ depending on the soil water content curves. Finally, the saturated hydraulic diffusivity (D_0) was calculated according to Grelle et al. (2014) and Schilirò et al. (2015) using the formula below:

$$D_0 = \frac{K_s H}{S_y} \quad (5)$$

where K_s is the saturated hydraulic conductivity, H the average soil thickness (assumed constant and equal to 1.5 m for the whole study area) and S_y the specific yield that can be assumed equal to 0.34 for the analyzed soils according to Johnson (1967), Loheide II et al. (2005) and Schilirò et al. (2015). H is considered equal to 1.5 m in coherence with the above-mentioned borehole logs and the constant soil thickness under study.

In particular, several parametric analyses in saturated and unsaturated conditions were performed using different combinations of shear strength data and locations of water table in the buffer zone, cases S and U in table 3.

For both saturated and unsaturated conditions, all cases were implemented considering the average values of hydraulic parameters. Particularly, in saturated condition, $K_s=1.79E-05$ m/s, $D_0=7.92E-05$ m²/s and $\theta_s=0.39$ were assumed; in unsaturated condition, the same hydraulic parameters as saturated plus residual volumetric water content $\theta_r=0.042$ and the parameter $\alpha=11.7$ were considered in order to approximate the soil-water characteristic curve for wetting the unsaturated soil (Gardner, 1958).

With reference to shallow landslide inventory, it is worth highlighting that the multi-temporal shallow landslide map used for the evaluation of the performance of TRIGRS analyses was obtained by combining the information provided by Giofrè et al. 2016 (dated 2001 and 2005) with landslide inventories provided by the Calabria region (dated 2001 and 2016) and the sliding scarps identified by Bonavina et al. (2005) and Moraci et al. (2017).

Regarding the official landslide inventories of the Calabria region, in the inventory only phenomena classified as debris flows or complex shallow phenomena were considered, and the sliding scarps were transformed into circles starting from crowns, in GIS environment.

Tables 4 and 5 report a summary of obtained results, listed in crescent order of EI, and the values assumed by the two statistics true positive fraction (TPF) and forecasting index (FI).

In saturated conditions (table 4); TPF values range from 94.1% (Cases 17S and 15S) to 52.9% (case 1S) and FI ranges from 31.4% (Cases 17S and 15S) to 13% (case 1S). The values assumed by TPF are complementary to EI, while the values assumed by FI indicate that an area going from 31.4% to 13% (depending on cases of analysis), at present not affected by shallow landslides (following the available landslide inventory), might be susceptible to shallow landslide triggering in the future. In unsaturated conditions (table 5), the values of FI range from 26.5% (Case 17U) to 6.2% (Case 1U) showing the capability of TRIGRS to take into account the effect of suction on slope stability (reducing the areas considered susceptible to shallow landslides).

The overall parametric analyses were implemented considering: i) a constant value of soil thickness, equal to 1.5 m of depth from the ground surface; ii) the average value of hydraulic data; and iii) an initial steady state water table located

This is a post-peer-review, pre-copyedit version of an article published in journal Landslide. The final authenticated version is available online at <https://doi.org/10.1007/s10346-018-1072-3>

at the bedrock–soil interface, in the whole study area, except in the road buffer zone (Zone A in figure 5). The best results, in terms of the smallest value of EI and the highest value of TPF, were obtained by the first group of analyses (cases 17, 15 and 13) in saturated as well as in unsaturated conditions. This group was carried out considering the average value of cohesion ($c'=2.5$ kPa) and the minimum value of shear strength angle ($\phi'=30^\circ$). The difference between the examined cases is due to the location of the initial water table in the road buffer zone (constituted by three contour lines, each equal to 5 m, from the secondary road) located at a depth of 0 m (case 17), 0.5 m (case 15) and 1.5 m (case 13), respectively. So doing, the first group of analyses shows values of $EI < 8\%$ in saturated and $EI < 13\%$ in unsaturated conditions.

In particular, cases 17S and 15S show $EI=5.9\%$ and TPF values equal to 94.1%, thus proving the ability of the model to analyze more than 90% of the area affected by the phenomena which occurred from 2001 to 2016. FI values are, in both cases, equal to 31.4%, thus suggesting that 31.4 % of the study area, unaffected by landslides until now, could be susceptible to landslides in the future.

In unsaturated conditions, cases 17U and 15U show $EI = 10.2\%$ (case 17U) and $EI=10.4\%$ (case 15U), the TPF values are equal to 89.8% (case 17U) and 89.6% (case 15U). FI values change from 31.4% (in saturated condition) to 26.5% (in unsaturated condition), showing that 26.5 % of the study area could be susceptible to landslides in the future.

Case 13 in tables 4 and 5 shows values of EI ranging from 7.6% (in saturated condition) to 12.4 (unsaturated), TPF values are 92.4% (saturated) and 87.6% (unsaturated) and FI changes from 31.2% (saturated) to 26.3% (unsaturated).

The second group of analyses (cases 12S, 8S and 4S) (Tab. 4) was carried out considering saturated conditions, the minimum value of cohesion ($c'=0$ kPa) and the average value of shear strength angle ($\phi'=38^\circ$). The results show values of EI ranging from 11.5% to 13.8%. These values are higher than those obtained from the previously described cases (17S, 15S and 13S) but are lower than 15% thus proving the ability of the analyses to predict more than 85% of unstable areas, as reported by TPF results equal to 88.5% (case 12S), 88.3% (case 8S) and 86.2% (case 4S). In unsaturated conditions, cases 12U, 8U and 4U (Tab. 5) show values of EI ranging from 20.0% to 22.6%, far higher than those obtained from cases 17U and 15U.

The poorest analyses were in Cases 9, 5 and 1, carried out considering the average value of cohesion and shear strength angle ($c'=2.5$ kPa, $\phi'=38^\circ$). In saturated conditions, these results show values of EI equal to 43.6% (case 9S), 44.7% (case 5S) and 47.1% (case 1S). In unsaturated conditions, EI values become 68.6% (case 9U), 70.1% (case 5U) and 73.9% (case 1U). These EI values are higher than those obtained for cases 17, 15 and 13 (both in saturated and unsaturated conditions).

The comparison of results shows that A_{UTL} , areas computed as unstable located within the A_{TL} (observed source areas), assumes, in saturated conditions, values greater than those obtained in unsaturated. Thus, EI (equation 3) decreases and, as a result, TPF increases.

In unsaturated conditions, for cases 10U, 6U, 2U, 9U, 5U, 1U implemented considering cohesion values equal to 2 kPa and 2.5 kPa and shear strength angle equal to 38° , TPF becomes less than 40% and EI is always equal or higher than 60% (Fig. 6c, d). However, for this study, it was decided that error index values above 20% (and then $TPF > 80\%$) cannot be accepted because a well-calibrated susceptibility map should be capable of predicting at least 80% of the observed landslides. This value is far higher than the threshold of $TPF=50\%$ proposed by Fressard et al. (2014).

Focusing on the results obtained in saturated conditions, it is worth highlighting that cases 13S ($c'=2.5$ kPa and $\phi'=30^\circ$) and 4S ($c'=0$ kPa and $\phi'=38^\circ$), implemented considering a water table located at a depth of 1.5 m from the ground surface, only partially analyze the landslides of 12th May 2001 (Fig. 7a). On the contrary, cases 17S and 12S, implemented considering the same geotechnical properties but a water table located at 0 m from the ground surface, can analyze the two landslide triggerings which took place on 2001 (Fig. 7b).

Therefore, Fig. 7 clearly highlights that if the water table located near the ground surface in the secondary road buffer zone (e.g., 0 m from the ground surface – case 17S and 12S, Fig. 7b) is not considered, one of the phenomena which occurred in 2001 cannot be analyzed by the model (Fig. 7a). This is due to the significant role played by the secondary road which, during the landslide event, channeled a greater quantity of water into the buffer zone, as already suggested by Antronico et al. (2006) and Bonavina et al. (2005).

According to principle that future landslides are likely to occur in the same geological, geomorphological and hydrological contexts that produced instability in the past up to the present, the map showing the lowest value of EI was considered the most representative susceptibility map for shallow landslides in the area (Fig. 8). Considering that two cases present the same value of EI, cases 17S and 15S, the overall accuracy of the best tests is evaluated by the ROC curves and the area under the ROC curves (AUC). ROC curves plot “sensitivity” on the Y axis versus “1-specificity” on the X axis (Metz 1978; Swets 1988); an AUC of 1 represents a perfect test. According to Fressard et al. (2014), AUC values less than 0.7 are indicative of a poor performance, values ranging from 0.7 to 0.8 represent a fair performance of the model, values between 0.8 and 0.9 reflect a good performance and over the threshold of 0.9, the predictive ability of the model can be considered excellent. In literature, few papers report AUC values higher than 0.80 (e.g., Schilirò et al. 2016; Ciarleo et al. 2017) for landslide susceptibility and hazard assessed by physically-based models. The obtained AUC values are 86.32% (case 17S) and 86.16% (case 15S) thus demonstrating a good performance of the model.

Case 17S is considered the best map because it shows the lowest value of $EI=5.9\%$ and the highest value of $AUC=86.32\%$ (Fig. 8). It was obtained using: i) the average value of cohesion and the minimum value of shear strength angle, ii) the

This is a post-peer-review, pre-copyedit version of an article published in journal *Landslide*. The final authenticated version is available online at <https://doi.org/10.1007/s10346-018-1072-3>

average value of hydraulic parameters and iii) a water table located at 0 m from the ground surface in the secondary road buffer zone and 1.5 m from the ground surface in the remaining study area.

Regarding the obtained FI value (31.4%) for case 17S, it is noted that 31.4% of the study area is susceptible to shallow landslide triggering events in the future.

5. CONCLUDING REMARKS

The obtained results show the ability of TRIGRS to predict shallow landslide source areas especially when few detailed geotechnical input data are available. For the analyzed case study and on the basis of the available input data, the examination of saturated and unsaturated results shows that the saturated results seem to be more coherent with the shallow landslide source areas which occurred on the Favazzina slopes. Indeed, values of AUC higher than 80% demonstrate the good forecasting ability of the obtained shallow landslide susceptibility map. This result could be further improved with detailed in situ investigation and laboratory tests. These in-depth analyses will allow us to better characterize the mechanical and hydraulic properties of weathered gneiss, especially in unsaturated conditions, thus defining a more detailed geotechnical model of slopes. Once a detailed geotechnical slope model has been formulated, the ability of TRIGRS to take into account both the transient pore-water pressure regime and the unsaturated conditions (Savage et al. 2004; Baum et al. 2008) characterizing different soils should be tested in the study area in order to obtain more significant results.

The landslide susceptibility map can be considered a large scale quantitative map which can select more limited zones where the above-mentioned in situ investigations and laboratory tests should be carried out in order to then rigorously characterize shallow landslide source areas (especially in terms of volume) and use the physically-based models correctly for the analysis of the propagation phase. This could provide a quantitative assessment of debris flow susceptibility and hazard to design the most appropriate countermeasures.

Acknowledgments

All authors have contributed in equally to the development of the research and to the extension of memory.

REFERENCES

- Antronico L, Cotecchia F, Cotecchia V, Gabriele S, Gullà G, Iovine G, Lollino G, Moraci N, Pagliarulo R, Petrucci O, Rocca F, Sorriso-Valvo M, Terranova O (2006). Attività di monitoraggio di siti in frana e di aree soggette a fenomeni di subsidenza. POR Calabria 2000-2006.
- Baum RL, Savage WZ, Godt JW (2002). TRIGRS-A FORTRAN program for transient rainfall infiltration and grid-based regional slope-stability analysis. US Geological Survey Open-File Report 02-0424. Available via: <http://pubs.usgs.gov/of/2002/ofr-02-424/>
- Baum RL, Coe JA, Godt JW, Harp EL, Reid ME, Savage WZ, Schulz WH, Brien DL, Chleborad AF, Mckenna JP, Michael JA (2005). Regional landslide-hazard assessment for Seattle, Washington, USA. *Landslides*, 2(4): 266–279.
- Baum RL, Savage WZ, Godt JW (2008) TRIGRS-A Fortran program for transient rainfall infiltration and grid-based regional slope-stability analysis, version 2.0. US Geological Survey Open-File Report 2008–1159. Available from: <http://pubs.usgs.gov/of/2008/1159/>
- Bishop AW (1959). The principle of effective stress: *Teknisk Ukeblad*, 39: 859–863.
- Bonavina M, Bozzano F, Martino S, Pellegrino A, Prestininzi A, Scandurra R (2005). Le colate di fango e detrito lungo il versante costiero tra Bagnara Calabria e Scilla (Reggio Calabria): valutazioni di suscettibilità. *Giornale di Geologia Applicata*, 2: 65–74.
- Borrelli L, Ciurleo M, Gullà G (2018). Shallow landslide susceptibility assessment in granitic rocks using GIS-based statistical methods: the contribution of the weathering grade map. *Landslide*, 15: 1127–1142.
- Borrelli L, Coniglio S, Critelli S, La Barbera A, Gullà G (2016). Weathering grade in granitoid rocks: The San Giovanni in Fiore area (Calabria, Italy). *Journal of Maps*, 12: 260-275.
- Borrelli L, Critelli S, Gullà G, Muto F (2015). Weathering grade and geotectonics of the western-central Mucone River basin (Calabria, Italy). *Journal of Maps*, 11: 606-624.
- Borrelli L, Gioffrè D, Gullà G, Moraci N (2012). Suscettibilità alle frane superficiali veloci in terreni di alterazione: un possibile contributo della modellazione della propagazione. *Rendiconti Online Società Geologica Italiana*, 21: 534-536.
- Borrelli L, Perri F, Critelli S, Gullà G (2014). Characterization of granitoid and gneissic weathering profiles of the Mucone River basin (Calabria, southern Italy). *Catena*, 113: 325-340.

This is a post-peer-review, pre-copyedit version of an article published in journal *Landslide*. The final authenticated version is available online at <https://doi.org/10.1007/s10346-018-1072-3>

- Brabb E.E. (1984). Innovative approaches to landslide hazard and risk mapping. Proc. of the IV International Symposium on Landslides, Toronto, vol. 1, pp. 307–323.
- Calvello M, Ciurleo M (2016). Optimal use of thematic maps for landslide susceptibility assessment by means of statistical analyses: case study of shallow landslides in fine grained soils. In: Proceedings ISL 2016, Landslides and Engineered Slopes. Experience–Theory and Practice, Napoli, Italy, vol. 2. pp. 537–544 (ISBN: 978-1-138-02988-0).
- Calvello M, Cascini L, Mastroianni S (2013). Landslide zoning over large areas from a sample inventory by means of scale-dependent terrain units. *Geomorphology*, 182: 33–48.
- Calvello M, Cascini L, Sorbino G, Gullà G (2008). Soil suction modelling in weathered gneiss affected by landsliding. *Landslides and Engineered Slopes – Chen et al. (eds) © 2008 Taylor & Francis Group, London, ISBN 978-0-415-41196-7*.
- Cascini L, Gullà G, Sorbino G (2006). Groundwater modelling of a weathered gneissic cover. *Canadian Geotechnical Journal*, 43: 1153-1166.
- Ciurleo M, Calvello M, Cascini L (2016) Susceptibility zoning of shallow landslides in fine grained soils by statistical methods. *Catena*, 139: 250–264.
- Ciurleo M, Cascini L, Calvello M (2017) A comparison of statistical and deterministic methods for shallow landslide susceptibility zoning in clayey soils. *Engineering Geology*, 223: 71–81.
- Fell R, Corominas J, Bonnard C, Cascini L, Leroi E, Savage WZ, On behalf of the JTC-1 Joint Technical Committee on Landslides and Engineered Slopes, 2008. Guidelines for landslide susceptibility, hazard and risk zoning for land-use planning. *Engineering Geology* 102: 85–98.
- Ferranti L, Monaco C, Morelli D, Antonioli F, Maschio L (2008) Holocene activity of the Scilla Fault, Southern Calabria: Insights from coastal morphological and structural investigations. *Tectonophysics*, 453: 74–93.
- Fressard M, Thiery Y, Maquaire O (2014) Which data for quantitative landslide susceptibility mapping at operational scale: case study of the Pays d’Auge plateau hillslopes (Normandy, France). *Natural Hazards and Earth System Sciences*, 14: 569–588.
- Gardner WR (1958). Some steady-state solutions of the unsaturated moisture flow equation with application to evaporation from a water table. *Soil Science*, 85: 228–232.
- GCO (1988) Geoguide 3: Guide to rock and soil descriptions. Geotechnical Control Office (GCO), Civil Engineering Services Department, Hong Kong.
- Giofrè D, Mandaglio MC, di Prisco C, Moraci N (2017). Evaluation of rapid landslide impact forces against sheltering structures. *Rivista Italiana di Geotecnica*, 3: 79-91.
- Giofrè D, Moraci N, Borrelli L, Gullà G (2016) Numerical code calibration for the back analysis of debris flow runout in Southern Italy. *Landslides and Engineered Slopes. Experience, Theory and Practice: Proceedings of the 12th International Symposium on Landslides 2*, pp. 991-997.
- Godt JW, Baum RB, Savage WZ, Salciarini D, Schulz WH, Harp EL (2008) Transient deterministic shallow landslide modeling: requirements for susceptibility and hazard assessments in a GIS framework. *Engineering Geology*, 102: 214–226.
- Grelle G, Soriano M, Revellino P, Guerriero L, Anderson MG, Diambra A, Fiorillo F, Esposito L, Diodato N, and Guadagno FM (2014) Space-time prediction of rainfall-induced shallow landslides through a combined probabilistic/deterministic approach, optimized for initial water table conditions. *Bulletin of Engineering Geology and the Environment*, 73: 877–890. doi:10.1007/s10064-013-0546-8.
- Gullà G, and Sorbino G (1994) Considerazioni sulla permeabilità satura dei materiali di alterazione di origine gneissica. In Proceedings of the Symposium “Il ruolo dei fluidi nei problemi di ingegneria geotecnica”, Mondovì, Italy, 1: 85-99.
- Gullà G, and Sorbino G (1996) Soil suction measurements in a landslide involving weathered gneiss. *In Proceeding of the 7th ISL, Trondheim, Norway*, 2: 749–754.
- Gullà G, Mandaglio MC, Moraci N (2006) Effect of weathering on the compressibility and shear strength of a natural clay. *Canadian Geotechnical Journal*, 43 (6): 618-625.
- Gullà, G, Mandaglio MC, Moraci N (2005) Influence of degradation cycles on the mechanical characteristics of natural clays. *In Proceedings of the 16th International Conference on Soil Mechanics and Geotechnical Engineering: Geotechnology in Harmony with the Global Environment Volume 4, 2005*, pp 2521-2524.
- Hungr O, Picarelli L, Leroueil S (2014) The Varnes classification of landslides-an update. *Landslides* 11: 167-194.
- Iverson RM (2000) Landslide triggering by rain infiltration. *Water Resource Research* 36 (7): 1897–1910.
- Johnson AI (1967) Specific yield-compilation of specific yields for various materials, US Geological Survey, Water Supply Paper, 1662- D, 74 pp.
- Loheide II S P, Butler Jr. JJ, and Gorelick SM (2005) Estimation of groundwater consumption by phreatophytes using diurnal water table fluctuations: a saturated-unsaturated flow assessment. *Water Resource Research*, 41, W07030, doi:10.1029/2005WR003942.
- Mandaglio MC, Moraci N, Giofrè D, Pitasi A (2015) Susceptibility analysis of rapid flowslides in southern Italy. *In Proceedings of the International Symposium on Geohazards and Geomechanics, ISGG 2015, University of Warwick, United Kingdom, 10–11 September 2015. IOP Conference Series: Earth and Environmental Science*, 26.

This is a post-peer-review, pre-copyedit version of an article published in journal *Landslide*. The final authenticated version is available online at <https://doi.org/10.1007/s10346-018-1072-3>

- Mandaglio MC, Moraci N, Rosone M, Farulla CA (2016a) Experimental study of a naturally weathered stiff clay. *Canadian Geotechnical Journal*, 53 (12): 2047-2057.
- Mandaglio MC, Moraci N, Gioffrè D, Pitasi A (2016b) A procedure to evaluate the susceptibility of rapid flowslides in Southern Italy. *In Proceedings of 12th International Symposium on Landslides, Napoli, Italy, 12–19 June 2016. Landslides and Engineered Slopes, Experience, Theory and Practice*, 3: pp. 1339-1344.
- Metz CE (1978) Basic principles of ROC analysis. *Seminars in Nuclear Medicine*, 8: 283–298.
- Montgomery D.R., Dietrich W.E. 1994. A physically based model for the topographic control on shallow landsliding. *Water Resource Research*, 30: 1153–1171.
- Montrasio L, Valentino R, Losi GL (2011) Towards a real-time susceptibility assessment of rainfall-induced shallow landslides on a regional scale. *Natural Hazards and Earth System Sciences*, 11: 1927–1947. <http://dx.doi.org/10.5194/nhess-11-1927-2011>
- Moraci N, Mandaglio MC, Gioffrè D, Pitasi A (2017) Debris flow susceptibility zoning: an approach applied to a study area. *Rivista Italiana di Geotecnica*, 51(2).
- Salciarini D, Fanelli G, Tamagnini C (2017) A probabilistic model for rainfall—induced shallow landslide prediction at the regional scale. *Landslides*, DOI 10.1007/s10346-017-0812-0
- Salciarini D, Godt JW, Savage WZ, Conversini P, Baum R, Michael JA (2006) Modeling regional initiation of rainfall induced shallow landslides in the eastern Umbria Region of central Italy. *Landslides*, 3: 181–194.
- Savage WZ, Godt JW, Baum RL (2004) Modeling time-dependent areal slope stability. In: Lacerda WA, Erlich M, Fontoura SAB, Sayao ASF (eds) *Landslides-evaluation and stabilization, Proceedings of 9th International symposium on Landslides*, vol 1. Balkema, Rotterdam, pp 23–36.
- Schilirò L, Esposito C, Scarascia Mugnozza G (2015) Evaluation of shallow landslide triggering scenarios through a physically based approach: an example of application in the southern Messina area (northeastern Sicily, Italy). *Natural Hazards and Earth System Sciences*, 15: 2091–2109.
- Schilirò L, Montrasio L, Scarascia Mugnozza G (2016) Prediction of shallow landslide occurrence: Validation of a physically-based approach through a real case study. *Science of the Total Environment*, 569–570: 134–144.
- Sorbino G, Sica C, Cascini L (2010) Susceptibility analysis of shallow landslides source areas using physically based models. *Natural Hazards* 53: 313–332.
- Sorbino G, Sica C, Cascini L, Cuomo S (2007) On the forecasting of flowslides triggering areas using physically based models. In: *Proceedings of 1st North American Landslides Conference*, vol. 23. AEG Special Publication, pp. 305–315.
- Srivastava R, Yeh T-CJ (1991) Analytical solutions for one-dimensional, transient infiltration toward the water table in homogeneous and layered soils. *Water Resource Research* 27:753–762.
- Swets JA (1988) Measuring the accuracy of diagnostic systems. *Science* 240, 1285–1293.
- Taylor DW (1948) *Fundamentals of Soil Mechanics*: New York, Wiley, 700 p.
- Varnes D.J. (1984) Landslide hazard zonation: a review of principles and practice. *The International Association of Engineering Geology Commission on Landslides and Other Mass Movements. Natural Hazards* 3–63 (Paris, France. ISBN 92-3- 01895-7).

Tab. 1 – Geotechnical properties of weathered gneiss of class VI

REFERENCES	Gravel (%)	Sand (%)	Silt (%)	Clay (%)	γ_{sat} (kN/m ³)	c' (kPa)	φ' (°)
						0	38
Antronico et al. 2006	50.58	27.26	19.05	3.11	19.46– 21.98	0	44
						0	38
Schilirò et al. (2015)	24.2-58.1	27-52.5	5.9-15.3	1.1-8	19.22	0	30
						5	40

Tab. 2 – Hydraulic properties of weathered gneiss of class VI

REFERENCES	K_s (m/s)	θ_s (-)	θ_r (-)	D_0 (m ² /s)	α (m ⁻¹)
		0.40			
Antronico et al. (2006)		0.54			
	6.60E-05	0.38	0.05	1.55E-04	11.8
Schilirò et al. (2015)	1.25E-05	0.39	0.04	3.84E-04	11.1
	7.91E-06	0.38	0.04	2.43E-05	12.2
	1.27E-06	0.32			
Calvello et al. (2008)	8.10E-06	0.32			
	2.78E-06	0.35			
Cascini et al. (2006)	3.50E-05				
Gullà and Sorbino (1994)	1.00E-05				

Tab. 3 – Input data used in TRIGRS in saturated and unsaturated conditions.

TRIGRS					TRIGRS unsaturated				
CASE*	WATER TABLE IN THE ZONE "A" (m)	WATER TABLE IN THE ZONE "B" (m)	c' (kPa)	ϕ' (°)	CASE*	WATER TABLE IN THE ZONE "A" (m)	WATER TABLE IN THE ZONE "B" (m)	c' (kPa)	ϕ' (°)
1S	1.5	1.5	2.5	38	1U	1.5	1.5	2.5	38
2S	1.5	1.5	2	38	2U	1.5	1.5	2	38
3S	1.5	1.5	1	38	3U	1.5	1.5	1	38
4S	1.5	1.5	0	38	4U	1.5	1.5	0	38
5S	0.5	1.5	2.5	38	5U	0.5	1.5	2.5	38
6S	0.5	1.5	2	38	6U	0.5	1.5	2	38
7S	0.5	1.5	1	38	7U	0.5	1.5	1	38
8S	0.5	1.5	0	38	8U	0.5	1.5	0	38
9S	0.0	1.5	2.5	38	9U	0.0	1.5	2.5	38
10S	0.0	1.5	2	38	10U	0.0	1.5	2	38
11S	0.0	1.5	1	38	11U	0.0	1.5	1	38
12S	0.0	1.5	0	38	12U	0.0	1.5	0	38
13S	1.5	1.5	2.5	30	13U	1.5	1.5	2.5	30
14S	1.5	1.5	2.5	34	14U	1.5	1.5	2.5	34
15S	0.5	1.5	2.5	30	15U	0.5	1.5	2.5	30
16S	0.5	1.5	2.5	34	16U	0.5	1.5	2.5	34
17S	0.0	1.5	2.5	30	17U	0.0	1.5	2.5	30
18S	0.0	1.5	2.5	34	18U	0.0	1.5	2.5	34

* S = saturated, U = unsaturated

Tab. 4 – Input data and values of indexes used in saturated conditions to evaluate the reliability of TRIGRS for susceptibility analyses.

CASE	WATER TABLE IN THE ZONE "A" (m)	WATER TABLE IN THE ZONE "B" (m)	c' (kPa)	ϕ' (°)	TPF (%)	FI (%)	EI (%)
17S	0.0	1.5	2.5	30	94.1	31.4	5.9
15S	0.5	1.5	2.5	30	94.1	31.4	5.9
13S	1.5	1.5	2.5	30	92.4	31.2	7.6
12S	0.0	1.5	0	38	88.5	25.7	11.5
8S	0.5	1.5	0	38	88.3	25.6	11.7
4S	1.5	1.5	0	38	86.2	25.5	13.8
18S	0.0	1.5	2.5	34	84.3	23.1	15.7
16S	0.5	1.5	2.5	34	84.0	23.0	16.0
14S	1.5	1.5	2.5	34	81.9	22.8	18.1
7S	0.5	1.5	1	38	79.4	21.3	20.6
11S	0.0	1.5	1	38	79.3	22.8	20.7
3S	1.5	1.5	1	38	76.5	21.0	23.5
10S	0	1.5	2	38	63.2	16.0	36.8
6S	0.5	1.5	2	38	62.1	15.9	37.9
2S	1.5	1.5	2	38	60.3	15.7	39.7
9S	0.0	1.5	2.5	38	56.4	13.3	43.6
5S	0.5	1.5	2.5	38	55.3	13.2	44.7
1S	1.5	1.5	2.5	38	52.9	13.0	47.1

Tab. 5 – Input data and values of indexes used in unsaturated conditions to evaluate the reliability of TRIGRS for susceptibility analyses.

CASE	WATER TABLE IN THE ZONE "A" (m)	WATER TABLE IN THE ZONE "B" (m)	c' (kPa)	ϕ' (°)	TPF (%)	FI (%)	EI (%)
17U	0.0	1.5	2.5	30	89.8	26.5	10.2
15U	0.5	1.5	2.5	30	89.6	26.5	10.4
13U	1.5	1.5	2.5	30	87.6	26.3	12.4
12U	0.0	1.5	0	38	80.0	21.6	20.0
8U	0.5	1.5	0	38	79.7	21.5	20.3
4U	1.5	1.5	0	38	77.4	21.3	22.6
18U	0.0	1.5	2.5	34	62.8	15.9	37.2
16U	0.5	1.5	2.5	34	62.2	15.8	37.8
11U	0.0	1.5	1	38	61.1	15.0	38.9
7U	0.5	1.5	1	38	60.4	14.9	39.6
14U	1.5	1.5	2.5	34	59.6	15.6	40.4
3U	1.5	1.5	1	38	58.0	14.7	42.0
10U	0.0	1.5	2	38	40.1	9.0	59.9
6U	0.5	1.5	2	38	38.9	8.9	61.1
2U	1.5	1.5	2	38	35.9	8.6	64.1
9U	0.0	1.5	2.5	38	31.4	6.6	68.6
5U	0.5	1.5	2.5	38	29.9	6.5	70.1
1U	1.5	1.5	2.5	38	26.1	6.2	73.9

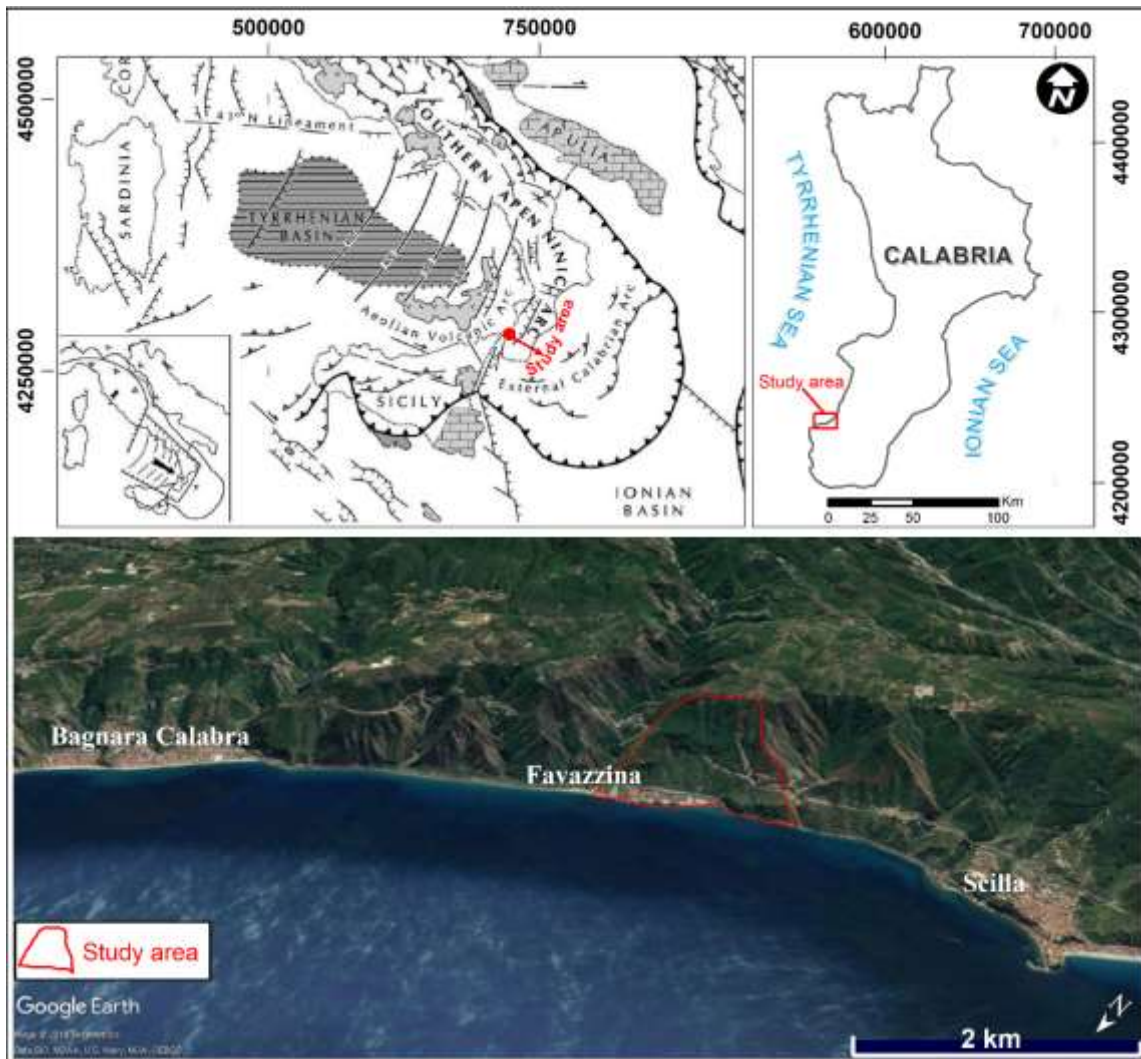


Fig. 1 – Geostructural and geographical localization of the study area.

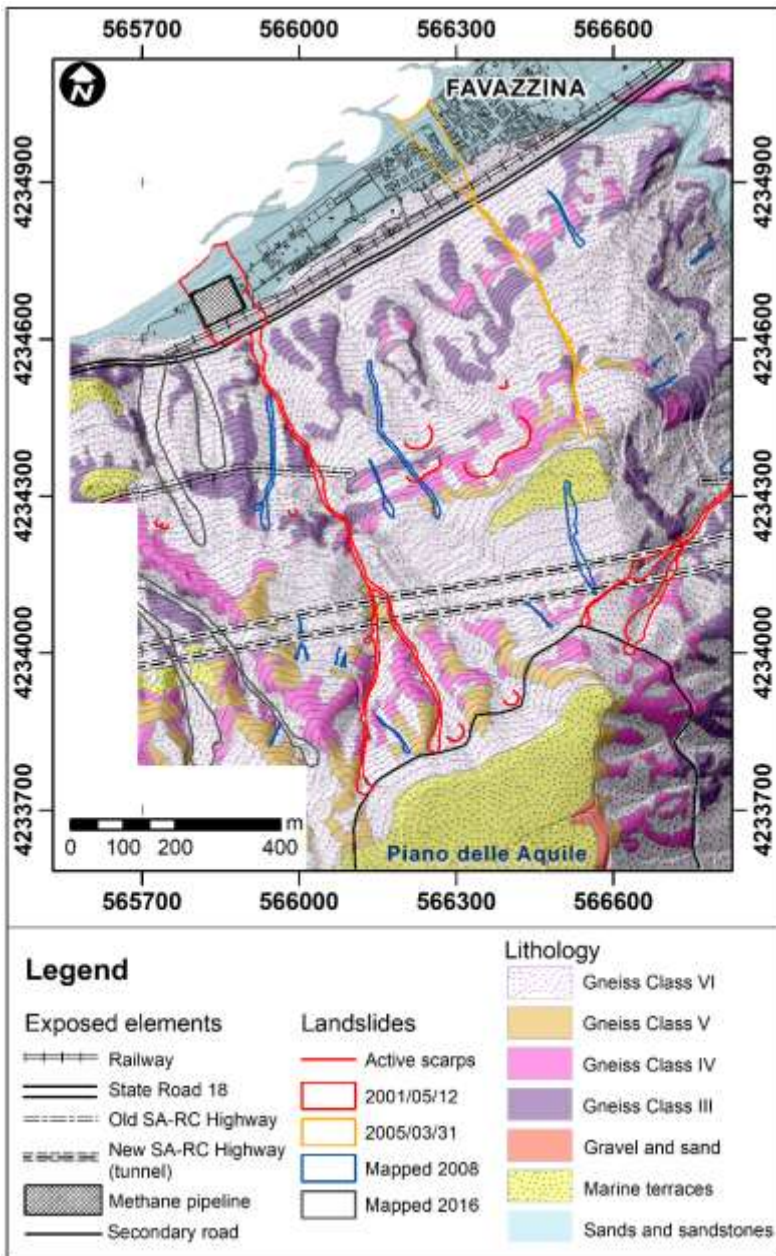


Fig. 2 – Lithological and weathering grade map of the Favazzina slopes.

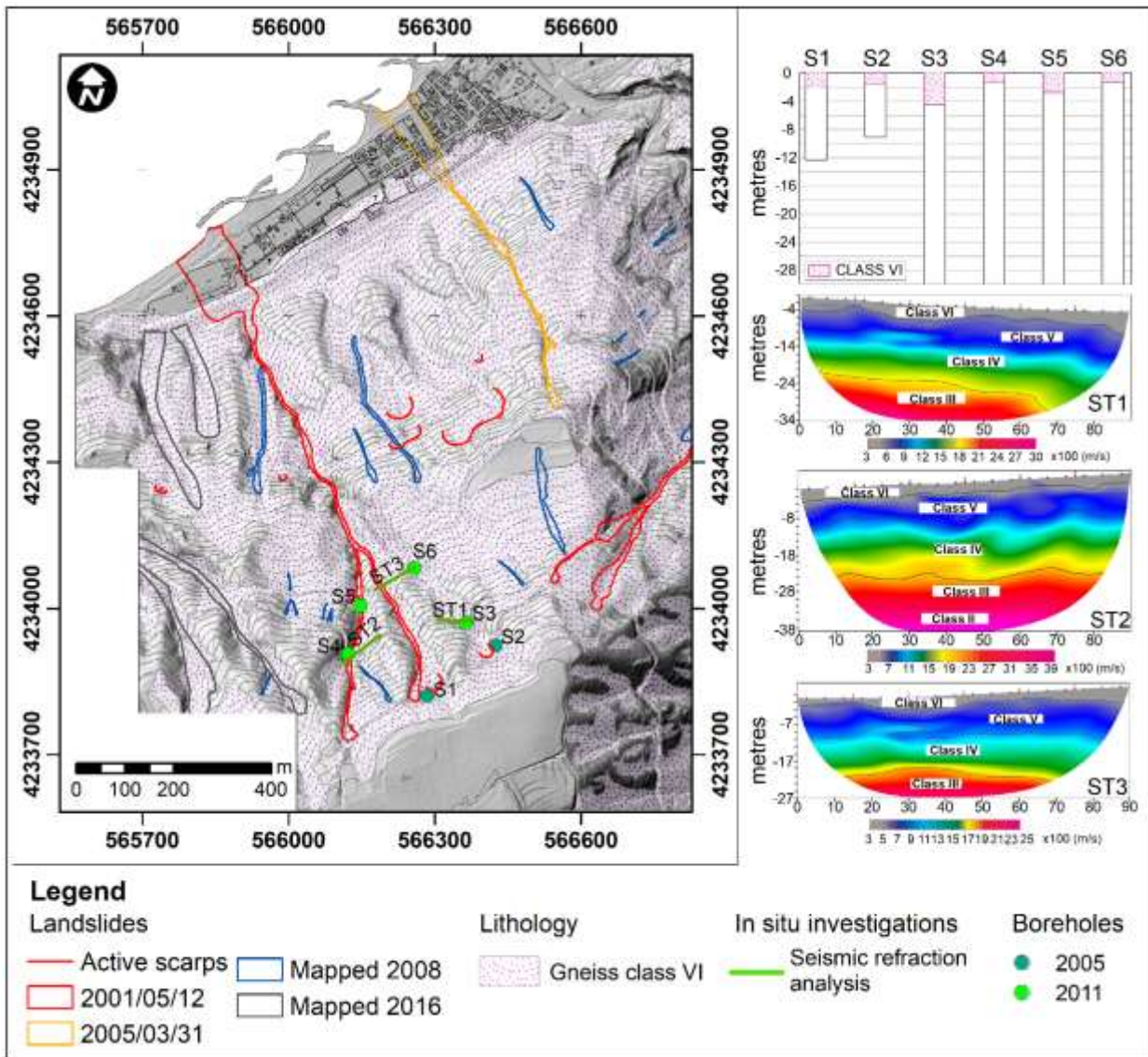


Fig. 3 – Landslide inventory and in situ investigations.

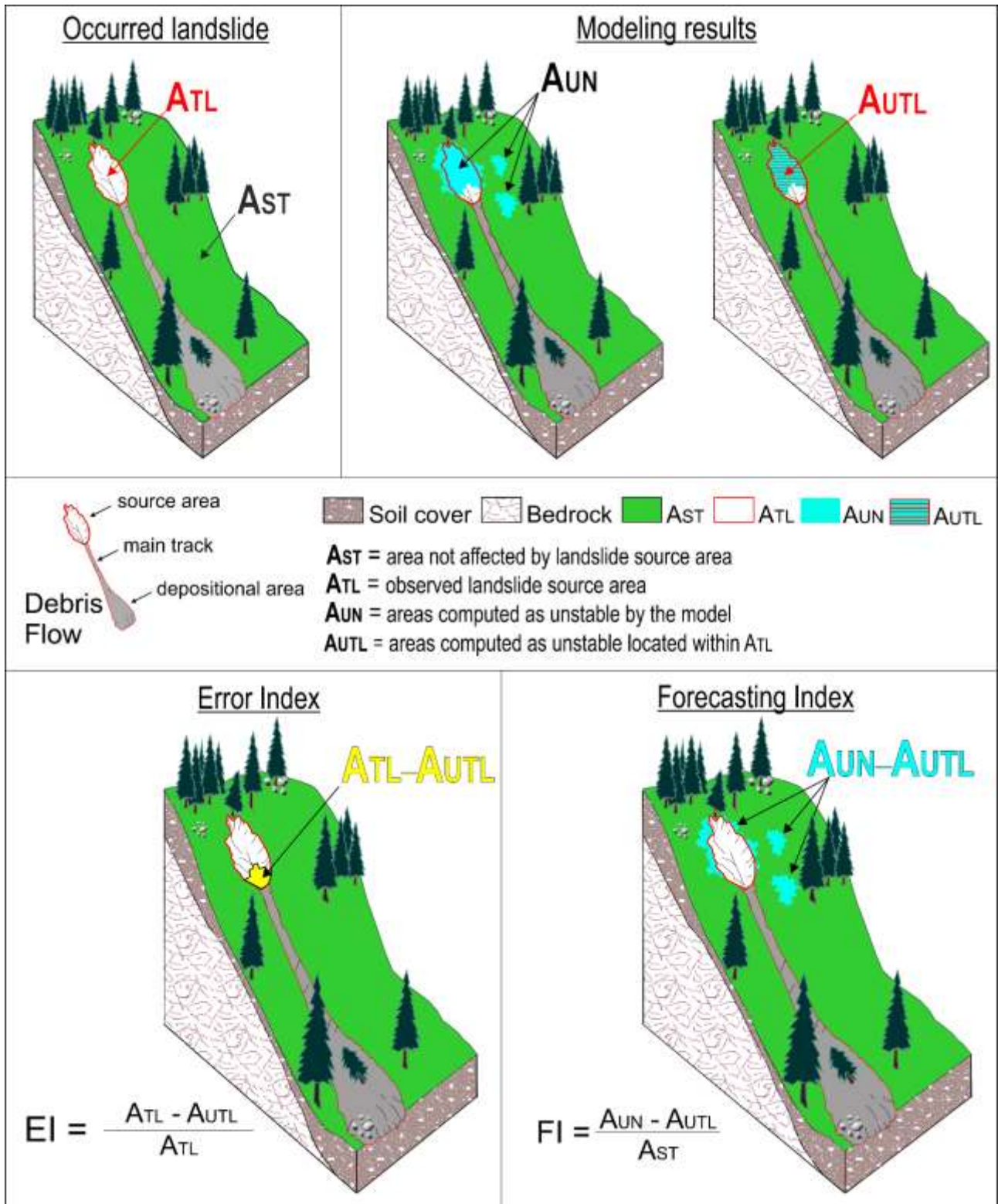


Fig. 4 – Indexes used to quantify the obtained results.

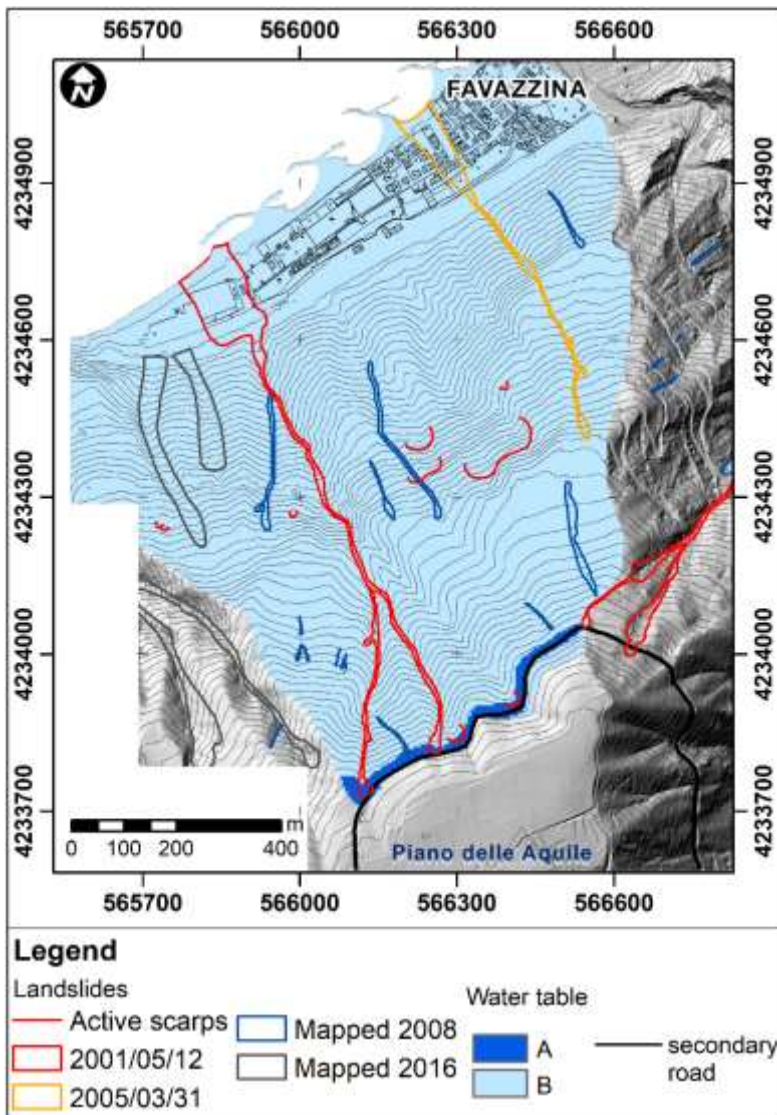


Fig. 5 – Initial water table locations. Legend: A=0 m, 0.5 m or 1.5 m from the ground surface; B= 1.5 m from the ground surface.

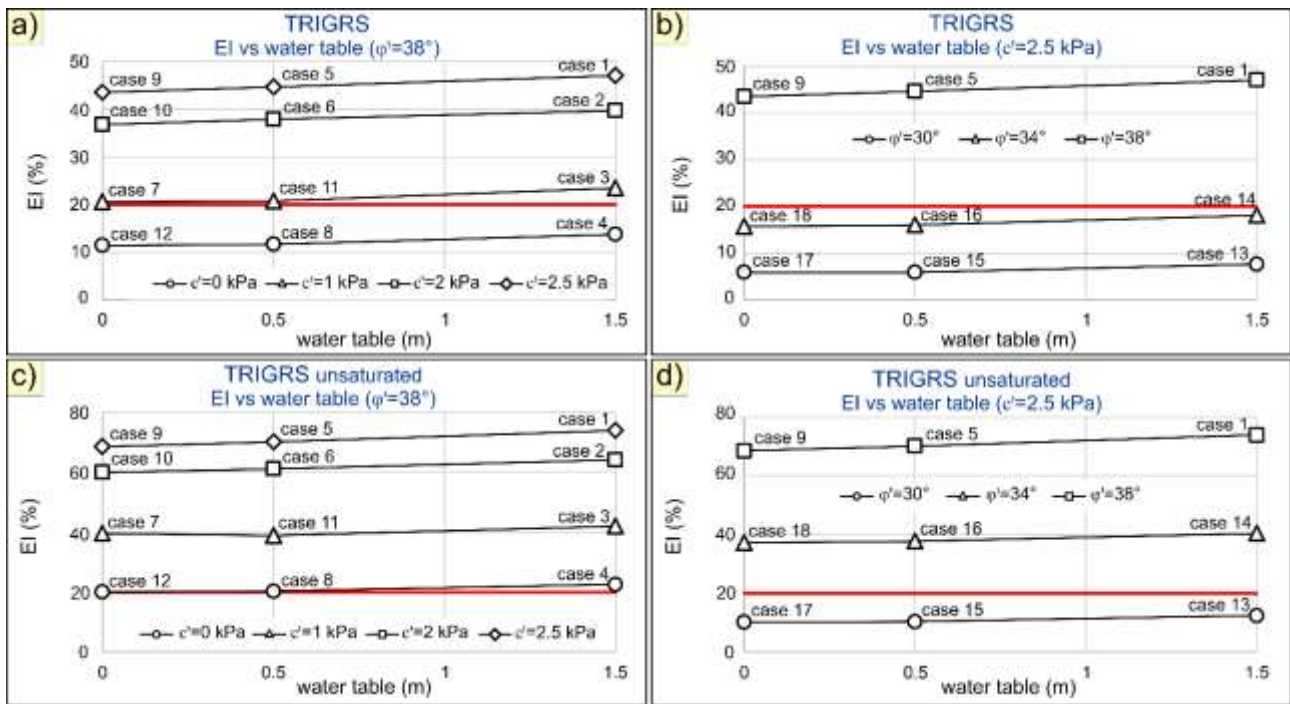


Fig. 6 – EI versus water table. a) results obtained considering saturated condition for $\phi' = 38^\circ$ and c' varying from 0 kPa to 2.5 kPa; b) results obtained considering saturated condition for $c' = 2.5$ kPa and ϕ' varying from 30° to 38° ; c) results obtained considering unsaturated condition for $\phi' = 38^\circ$ and c' varying from 0 kPa to 2.5 kPa; d) results obtained considering unsaturated condition for $c' = 2.5$ kPa and ϕ' varying from 30° to 38° . Each symbol/point in the graph represents a different implemented case.

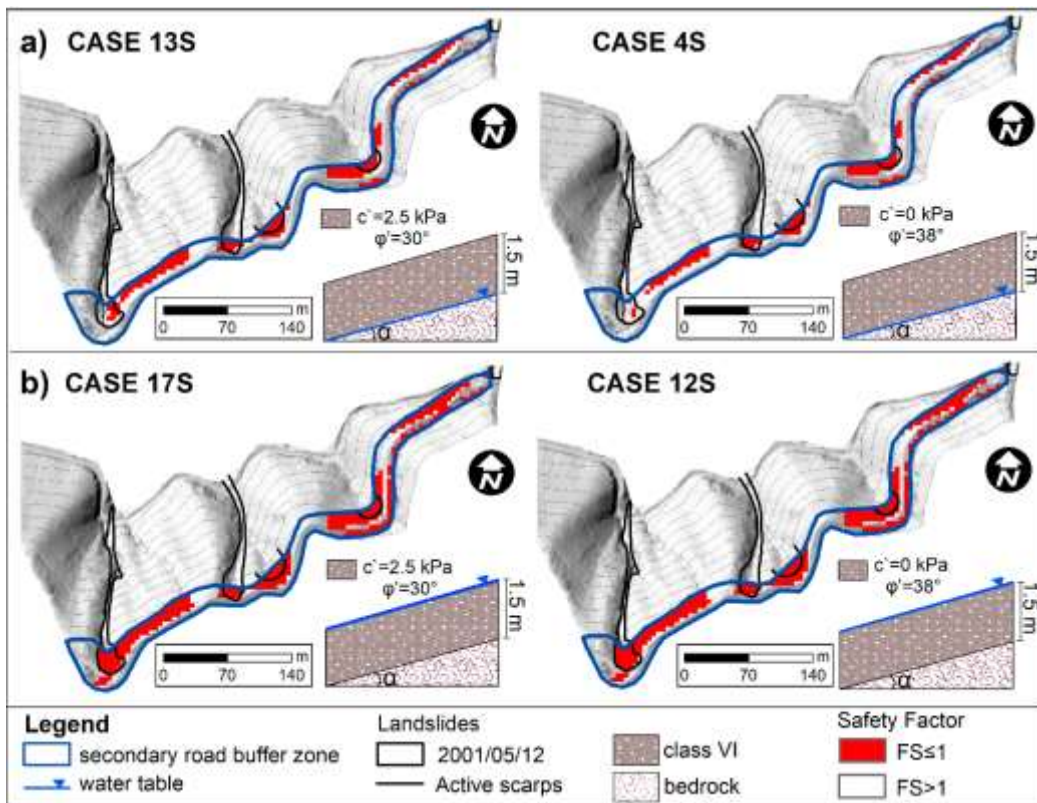


Fig. 7 – Comparison between the results obtained by TRIGRS for cases 13S, 4S and 17S, 12S in the upper part of the Favazzina slope. a) water table located at 1.5 m from the ground surface in the whole study area; b) water table located at 0 m from the ground surface in the secondary road buffer zone. Legend: α is the slope angle and it changes cell by cell.

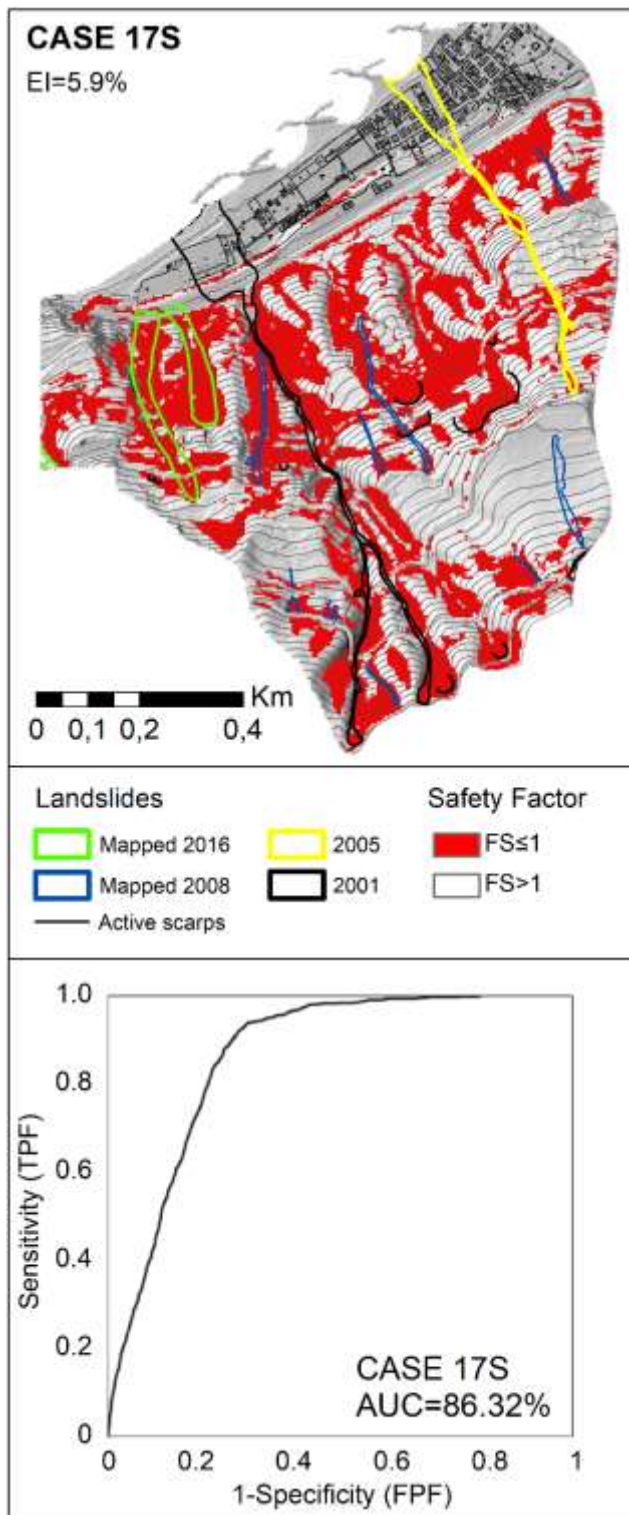


Fig. 8 – Landslide susceptibility computational map; receiver operating characteristic curve and AUC value.